

EFFECTS OF CROSS CORRELATED COVARIANCE ON SPACE-CRAFT COLLISION PROBABILITY

Vincent T. Coppola¹, James Woodburn², and Richard Hujsak³

The most widely used algorithm for computing spacecraft collision probability between two objects utilizes the relative position pdf derived from the relative position covariance. It is usually assumed that the position uncertainties are uncorrelated between the two objects---that is, there is no cross correlation contribution to the relative position covariance. This paper examines the sensitivity of the computed collision probability to non-zero cross correlation. In certain cases, small but physically realistic cross correlation may lead to large variations in collision probability. We will present an example wherein the cross correlation is computed through the use of a filter which simultaneously estimates the orbits of the two objects.

INTRODUCTION

In recent years, the computation of spacecraft collision probability has received considerable attention. An excellent discussion of the modeling assumptions and the standard computation can be found in a paper by Ken Chan (Ref. 1). We will be using Chan's analytical expressions to compute the probability of collision in this paper. Of critical importance to the computation is the pdf derived from the relative position covariance. In many cases, the uncertainty of the covariance itself is at issue: if the positional uncertainty is very large, then the resulting probability of collision will be very low, leading to a false sense of security. This aspect of the sensitivity of the computation to the input data has been investigated by Sal Alfano (Ref. 2). Akella and Alfriend (Ref. 3) have investigated variations of the standard assumptions to account for the uncertainty of the time of close approach. Glenn Peterson (Ref. 4) has investigated the effect of large relative velocity uncertainty on probability computations. Ken Chan (Ref. 5) investigates a method for computing collision probability when the standard assumption of large relative velocity does not hold. In each of these cases, the modeling assumptions and data incorporated by the standard algorithm are being exercised to determine its limitations, so that a meaningful result can be obtained, not just a mathematically correct one.

In this same vein, we investigate the effects of non-zero cross correlation on the relative position covariance. The standard assumption is that the two objects' position

¹ Member AAS and AIAA. Senior Astrodynamics Engineer, Analytical Graphics, Inc., 40 General Warren Blvd., Malvern, PA 19355, vcoppola@stk.com

² Member AAS and AIAA. Chief Orbital Scientist, Analytical Graphics, Inc., 40 General Warren Blvd., Malvern, PA 19355, woodburn@stk.com

³ Member AAS and AIAA. Senior Astrodynamics Engineer, Analytical Graphics, Inc., 40 General Warren Blvd., Malvern, PA 19355, rhujsak@stk.com

covariances are uncorrelated. If the orbit determination process is performed for each object separately, then the extent to which their states may be correlated is unknown. Correlation of the state estimates of the two objects becomes non-zero during simultaneous processing due to the estimation of common force model parameters, common tracking system biases or the processing of measurements which explicitly depend on the states of both objects. We will investigate cases where common tracking system biases are estimated and satellite to satellite measurements are considered. The estimation of corrections to a global atmospheric density model would be an example of estimating common force model parameters which could be investigated in a future study.

For a meaningful investigation, one needs to use physically reasonable values of the cross correlation. We will produce this data for a specific example conjunction using the orbit determination software package, STK/OD. STK/OD uses a sequential filter (Ref. 6) which can simultaneously estimate the orbits of the two objects, force modeling parameters for the satellites and measurement system biases. STK/OD also employs physically connected process noise models during the propagation of the covariance resulting in realistic covariance. The relative position covariance is constructed from the complete state estimate covariance. We will compare the probability of collision values when relative position covariance is computed with and without the cross correlation.

RELATIVE POSITION COVARIANCE

The computation of the relative position covariance is straight forward. Let x_A denote the position vector of object A; let x_B denote the position vector of object B; let $Dx = x_A - x_B$ denote the relative position vector. The relative position covariance P_{DD} is defined to be

$$P_{\Delta\Delta} = E[d(\Delta x)d(\Delta x)^T] = E[dx_A dx_A^T + dx_B dx_B^T - dx_A dx_B^T - dx_B dx_A^T] \quad (1)$$

where $E[\cdot]$ denotes the expectation operator. Using the linearity of $E[\cdot]$, we find

$$P_{\Delta\Delta} = P_{AA} + P_{BB} - (P_{BA} + P_{BA}^T). \quad (2)$$

where

$$P_{AA} = E[dx_A dx_A^T] \quad , \quad P_{BB} = E[dx_B dx_B^T] \quad , \quad P_{BA} = E[dx_B dx_A^T] \quad (3)$$

Figure 3 shows two objects at a close approach surrounded by their position covariance ellipsoids. The relative position covariance ellipsoid, computed using (3), is also shown centered at one of the objects. Note that the elongation of the relative covariance ellipsoid is much less than the elongations of the individual position covariances. This is expected whenever the symmetry axes do not align; in general, this is a common occurrence.

The relative position covariance matrix is used directly in the computation of collision probability. The standard assumption is then made that $P_{BA} = 0$, i.e., that the two objects' uncertainties are uncorrelated because of the unavailability of the cross correlation data. Moreover, zero seems to be a reasonable assumption in comparison with the worst case assumptions.

COLLISION PROBABILITY

We provide a very brief discussion of the collision probability computation. For a more complete discussion, see Chan (Ref. 1).

Consider the time of close approach between two objects involved in a conjunction. At this time, the range between the objects is at a minimum, which occurs when the relative position vector is perpendicular to the relative velocity vector. Consider a plane, called the encounter plane, whose normal is the relative velocity vector at the time of close approach. Since the relative position vector is perpendicular to the relative velocity vector at this time, the plane can be located to contain both objects. Define the y -axis along the relative velocity vector, the x -axis along the relative position vector, and the z -axis to complete the triad: then the encounter plane is the xz -plane.

Near the time of close approach it is assumed for modeling purposes that the motion of each object is a line. This is an accurate model for conjunctions of short duration, where the relative speed is not small and for objects that are meters in size rather than thousands of meters. This would not apply for objects in tight formations like co-located GEOs. The linear motion assumption permits a reduction from a three-dimensional pdf to a two dimensional pdf computed over an area in the encounter plane itself. The pdf in the encounter plane is given by

$$f(x, z) = \frac{1}{2ps_x s_z \sqrt{1 - r_{xz}^2}} e^{-\left[\left(\frac{x}{s_x}\right)^2 - 2r_{xz}\left(\frac{xz}{s_x s_z}\right) + \left(\frac{z}{s_z}\right)^2\right] / 2(1 - r_{xz}^2)} \quad (4)$$

where s_x , s_z , and r_{xz} describe the relative position covariance projected into the xz -plane. The probability of collision is then given by

$$P = \iint_A f(x, z) dx dz \quad (5)$$

where A is the collision cross-sectional area, typically (but not limited to) a circle.

Notice that the constant-probability curves of the pdf are ellipses in the xz -plane, whose major axis makes some angle θ to the x -axis, depending on ρ_{xz} . The integration is more easily computed by respecting the principal axes of these ellipses, by rotating to a new $x'z'$ axes system by θ and integrating in x' and z' .

The probability of collision is a function of just 5 parameters, shown in Table 1. The first parameter is a measure of the sizes of the objects; the second a measure of the nominal distance between the objects; the last three describe the projection of the relative covariance ellipsoid into the encounter plane. It is best to consider the analysis using non-dimensional variables. We use the following:

$$AR = \frac{S_{x'}}{S_{z'}} \quad , \quad H = \frac{r_A}{S_{z'}} \quad , \quad M = \frac{x_e}{S_{z'}} \quad , \quad \theta \quad , \quad (6)$$

where AR is the aspect ratio of the uncertainty ellipse in the encounter plane and is always greater or equal to 1, H is the hard body radius scaled by the minor uncertainty, M is the miss distance scaled by the minor uncertainty, and θ is already non-dimensional and lies between -90 and 90 deg.

Table 1

PARAMETERS FOR COMPUTING COLLISION PROBABILITY

Parameter	Description
r_A	Sum of hard body radii of primary and secondary
x_e	Miss distance (i.e., relative range between objects at TCA)
$S_{x'}$	Major axis of uncertainty ellipse in the encounter plane
$S_{z'}$	Minor axis of uncertainty ellipse in the encounter plane
θ	The angle between the line of sight between objects and the major axis of the uncertainty ellipse (x')

Chan makes a modeling assumption to transform the pdf integral from the (x', z') space into a scaled space (x'', z'') in which the integrand is isotropic, which then can be further transformed into an expression amiable for analytic approximation. His resulting analytic expression for P is then:

$$P \approx e^{-v/2} \left\{ 1 - e^{-u/2} + \frac{v}{2} \left[1 - \left(1 + \frac{u}{2} \right) e^{-u/2} \right] \right\} \quad (7)$$

$$\text{where } u = \frac{H^2}{AR} \quad \text{and} \quad v = M^2 \left(\sin^2(\mathbf{q}) + \frac{\cos^2(\mathbf{q})}{AR^2} \right) \quad (8)$$

The modeling assumption essentially assumes that AR is not too large. Chan was able to show cases where even for AR as large as 10, this approximate solution compares very favorably with others methods for integrating the pdf. We will be using (7) in our analysis, though the ultimate conclusions apply more generally than this specific approximation.

SENSITIVITY OF COLLISION PROBABILITY

Ultimately, the reason one computes the collision probability is to compare its value against a trigger threshold to make a decision about maneuvering. Values much larger than the trigger indicate a need for maneuver while values much smaller than the trigger indicate nothing to do. The calculation is only as good as the input data of course.

Of the five parameters from Table 1 that determine probability, r_A is the most likely quantity to be known with some confidence before an event. Miss distance depends on the nominal orbit predictions for both objects; these predictions may be refined over time leading to changing estimates of TCA and the miss distance itself. One's confidence in TCA and the encounter plane geometry is tied directly to the ephemeris predictions of the two objects, which in turn depend on such things as the time since orbit epoch and the ephemeris generation method (e.g., numerical integration, analytical approximation).

The probability calculation is most sensitive to the quality of the covariance. Sequential filters employ a structure that naturally allows for the addition of process noise during the propagation of covariance. The role of process noise is to increase the uncertainty due to the uncertainty in the dynamical model. Least squares methods lack a formal structure to account for dynamical modeling errors and typically employ empirically derived 'consider parameters' in an attempt to provide a realistic covariance.

Ultimately the covariance must be propagated to TCA and different error propagation may produce different predicted covariances at TCA. Lastly, although one's confidence in each objects' covariance may be high, the probability computation depends on the projection of the combined covariance ellipsoid into the encounter plane whose geometry is tied to TCA.

Given that the parameters needed for computing the probability are themselves uncertain, one should be cautious in making a decision based upon a value computed using nominal values. It would be prudent to determine the sensitivity of the computed probability to expected variations in the parameters describing the computation. As will

be seen, in some cases the probability is not sensitive to the variations in the parameter values, while in other cases it is sensitive. The real concern are times when the errors in the input parameters trigger a false alarm, or more seriously, fail to trigger an alarm when one is required.

The following analysis explores the sensitivity of the collision probability to errors in the covariance shape (AR) and orientation (θ).

Figure 1 shows a plot of probability as a function of θ , for 5 different AR values, at a fixed H and M . The figure shows the probability as two measures (θ , AR) of the relative covariance at TCA are varied while the geometry of the conjunction remains constant. Each curve is symmetric with respect to $\theta=0$ (which is also the maximum probability) and flattens out near $\theta= \pm 90$ deg. The curve is steepest somewhere in between (near $\theta=45$ deg, but the actual steepest point depends on AR). For a nominal value of θ near the steep part of the curve, a small variation in θ has a dramatic impact on the value of P .

Figure 2 shows a similar plot, for different values of H and M , corresponding to a larger scaled hard body radius and a larger scaled miss distance. The variations with θ and AR are similar to Figure 1, although the change in P for a change in a parameter is much more dramatic in this case. Notice, however, that while P is very sensitive to variations, it may be significantly less than the typical trigger value of 10^{-6} for a large range of θ .

As would be expected for a function of 4 variables, the two-dimensional plots do not completely characterize the variation of P to variations in each of its parameters. Moreover, it is unlikely that sweeping generalizations can be made, except for the few obvious ones (e.g., if the miss distance is large enough, the probability is always significantly lower than any (positive) trigger value). The two figures do demonstrate, however, that *there are areas within the parameter space where P is very sensitive to the values of the parameters*. Under these conditions, small errors in the input covariance can result in a large error in the probability.

SENSITIVITY OF PROBABILITY TO PREDICTION SPAN

Even in cases where the probability computation itself is not sensitive to parameter variations, the value of probability may vary as a result of improved data. Consider the case of two LEO objects, both 1 m in size, that have a close approach event.

We constructed a set of truth ephemerides which were used to produce simulated observations from the AFSCN tracking network in STK/OD. The STK/OD simulator was configured to generate time varying biases for each tracker/ measurement type combination and to add white noise to the measurements. Ground tracking observables consisted of two-way range, two-way Doppler, azimuth and elevation generated at a rate of one observation set per minute whenever the satellites were visible.

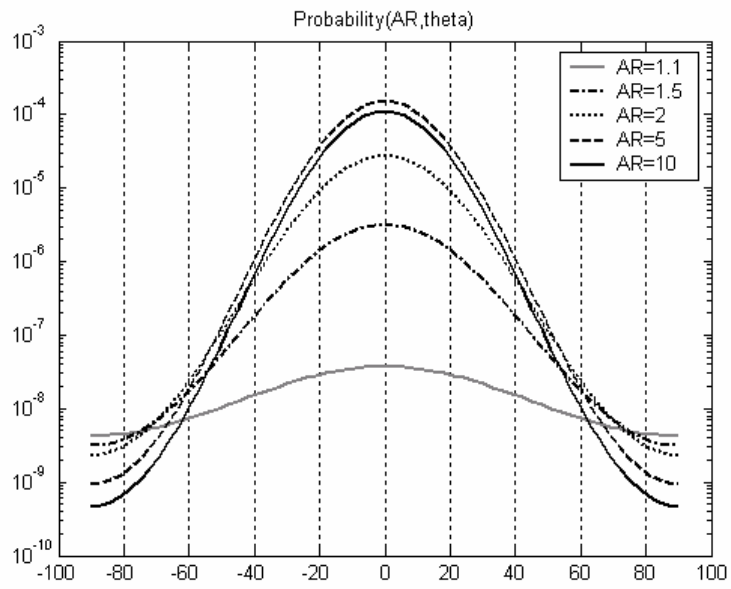


Figure 1. Probability as a function of θ , parameterized by AR , for $H=0.05$ and $M=5$.

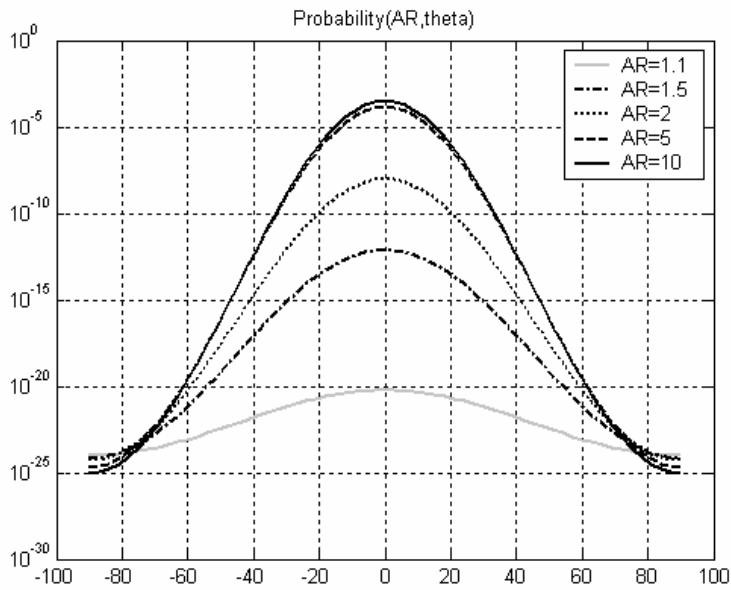


Figure 2. Probability as a function of θ , parameterized by AR , for $H=0.10$ and $M=10$.

The sequential filter in STK/OD was then used to simultaneously estimate the ephemeris and covariance of the two objects. Measurement processing was stopped at three times before the event and the trajectories and covariance were predicted to a time past the conjunction event to emulate an operational process of updating conjunction assessments as new tracking data becomes available. Three orbit determination solutions were computed: one with a 12 hour prediction span, one with a 6 hour span, and the last with a 3 hour span. For each case, we computed the predicted TCA and collision probability. As expected, the size of the relative covariance at TCA was smaller for the shorter predict spans.

Table 2 lists the various values used in the probability computation. In this particular example, the probability increased by a factor of 20 from the 12 hour predict to the 3 hour predict. The variability of the computed value is not a result of uncertain parameters but rather caused by the reduction of the relative covariance at TCA.

Table 2
PARAMETER VALUES FOR 3 PREDICTION SPANS

Parameter	12 hour	6 hour	3 hour
TCA diff (secs)	0.0137	0.0004	0.0013
x_e (m)	28.8	30.1	17.9
σ_z (m)	70.0	15.2	9.8
H	0.028	0.131	0.204
M	0.41	1.98	1.83
AR	1.1	2.68	2.12
θ (deg)	35.0	10.4	5.7
P	3.4e-04	2.3e-03	6.5e-03

CROSS CORRELATION

Typically, the correlation in position uncertainty between two objects is not known because each object's orbit determination is performed independently from all other objects. The correlation is then treated as zero in the computation of probability of collision. In many cases, such as space surveillance, the same algorithms, environmental force models, and tracking stations are used in the orbit determination for both objects, permitting the possibility that a non-zero cross correlation exists that is being ignored.

We used the results of the three OD runs from the previous section to determine the level of cross correlation in the position uncertainty of the two objects which would be introduced through the estimation of the common tracking system biases. We found that the cross-correlation could be quite significant, with the resulting relative position covariance ellipsoid being significantly affected in size and shape, see Figure 4.

High satellite-to-satellite cross correlations are developed during tracking by shared trackers with correlated bias errors. These cross correlations dissipate rapidly during prediction due to the continuing application of process noise for these parameters. Thus, the large cross correlation was found to be localized in time, near times of measurement updates. The cross correlation became insignificant at TCA.

This dissipation may be an artifice of continuous application of Gauss Markov stochastic model for biases. After all, if the bias states were dropped from state space at the end of the tracking pass, the satellite-to-satellite cross correlations would persist for a very long time. Tracking data occurs at discrete times, yet most sequential filters apply the bias process noise as a continuous process, and decorrelation during prediction is fairly standard. The authors plan to investigate the application of a discrete process noise model for bias states, and the consequences on collision probability, at a later date. Our expectation is that satellite to satellite correlations will remain high and will play a more important role in collision probability.

Space Based Measurements

We then investigated the use of satellite to satellite observations in the OD process. One vehicle measured the location of the other object and this ranging was used as part of the orbit determination of both objects simultaneously.

The test case cited in the previous section involves two LEO objects that have a repeating close approach every half revolution. We generated simulated satellite to satellite two-way range measurements at a frequency of one measurement every 5 seconds during two minute windows approximately centered on the conjunctions occurring 1 and 1.5 revolutions prior to the conjunction of interest. We processed that tracking data with STK/OD to produce a covariance with significant realistic cross correlation.

This models a case where one satellite had a limited ranging capability to better estimate the relative position covariance. Although this may not be realistic due to the high tracking rates during a conjunction, we use this example for illustrative purposes. These measurements produced a highly cross-correlated position covariance at the measurement time. Figure 5 depicts the relative position covariance ellipsoid just after a space based range measurement. The inclusion of cross correlation dramatically alters the ellipsoid. More importantly, a significant cross-correlation persisted for several revs after the measurement update.

The last space based measurement occurred 1 rev before the event. The relative position ellipsoid size at TCA, computed with and without the cross correlation, is given in Table 3. Figure 6 shows two views of the close approach event, showing the relative position covariance computed with and without the cross correlation. You can see that the two ellipsoids have different sizes and slightly different orientation and shape.

Table 3
RELATIVE POSITION COVARIANCE ELLIPSOID SIZE

Uncertainty	No cross correlation	With cross correlation
Maximum (m)	34.4	23.0
Middle (m)	18.0	16.2
Minimum (m)	9.6	9.9

Given that the ellipsoid size, shape, and orientation are different, and knowing that the probability may be sensitive to these variations, we computed the collision probability for both ellipsoids. Each object was assigned a finite size of 1m; the miss distance for the predicted ephemeris was 27 m. The relevant parameters are given in Table 4.

Table 4
PARAMETER VALUES FOR CASE UTILIZING SPACE-BASED MEASUREMENTS

Parameter	No cross correlation	With cross correlation
σ_z (m)	9.33	9.33
H	0.214	0.214
M	2.89	2.89
AR	1.58	1.63
θ (deg)	2.6	-1.3
P	2.7e-03	2.9e-03

In this example, the probabilities differ by just 7%. The value computed using the cross correlation is slightly higher than the value computed ignoring it, though the cross correlation ellipsoid is significantly smaller in size. The probability is not very sensitive to the size difference because the largest difference is in a direction mostly perpendicular to the encounter plane. This may be serendipity---if the largest difference had been in the encounter plane, then the different ellipsoids may lead to very different probabilities.

CONCLUSION

We have investigated position cross-correlation in several examples. We have shown that significant cross correlation can exist; however, it may dissipate quickly over time. We need to investigate further whether the fast dissipation is an artifact of the orbit determination modeling of biases. Our example using space based measurements produced a highly cross-correlated covariance at TCA. In such a case, the collision probabil-

ity computation should (and easily can) include the cross-correlation. Although ignoring the cross correlation in this example produced a similar value of collision probability, others examples may not. We have shown that there exists areas of the collision probability parameter space that are sensitive to parameter errors. The example happened to lie in an insensitive part of the parameter space.

REFERENCES

1. F. K. Chan, "Improved Analytical Expressions for Computing Spacecraft Collision probabilities," AAS 03-184, Ponce, Puerto Rico, February 2003.
2. S. Alfano. "Relating Position Uncertainty to Maximum Conjunction Probability", AASS 03-548, Big Sky, Montana, August 2003.
3. Akella, M. R. and Alfriend, K. T. "Probability of Collision between Space Objects", J. of Guidance, Control, and Dynamics, Vol 23. No 5, Sept-Oct 2000, pp769-772.
4. G. Peterson. "Effect of Large velocity Covariance on Probability Computations," AAS 03-552, Big Sky, Montana, August 2003.
5. F. K. Chan, "Spacecraft Collision probability for Long-term Encounters", AAS 03-549, Big Sky, Montana, August 2003.
6. J. R. Wright, "Optimal Orbit Determination", AAS 02-192, San Antonio, Texas, January 2002.

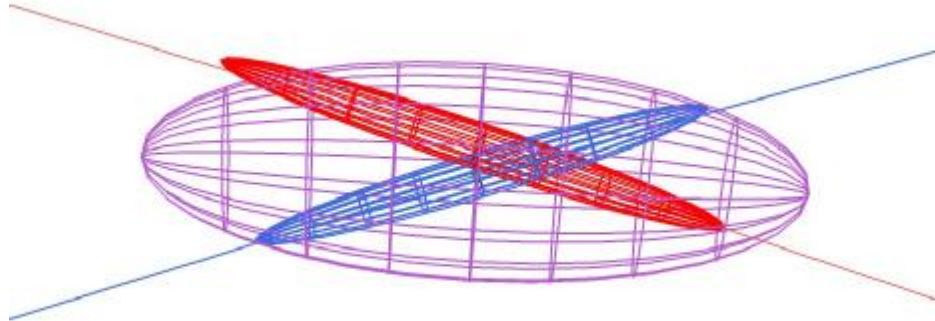


Figure 3. The position covariance ellipsoids are shown in red and blue. The relative position covariance ellipsoid is shown in purple.

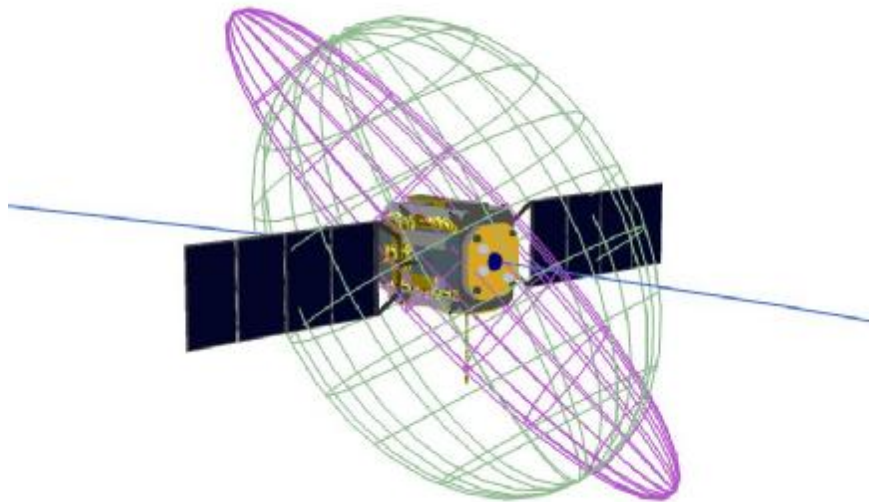


Figure 4. The relative position covariance ellipsoid, shown at a time just after a ground range measurement. The purple ellipsoid is computed with the cross correlation; the green one ignores the cross correlation.

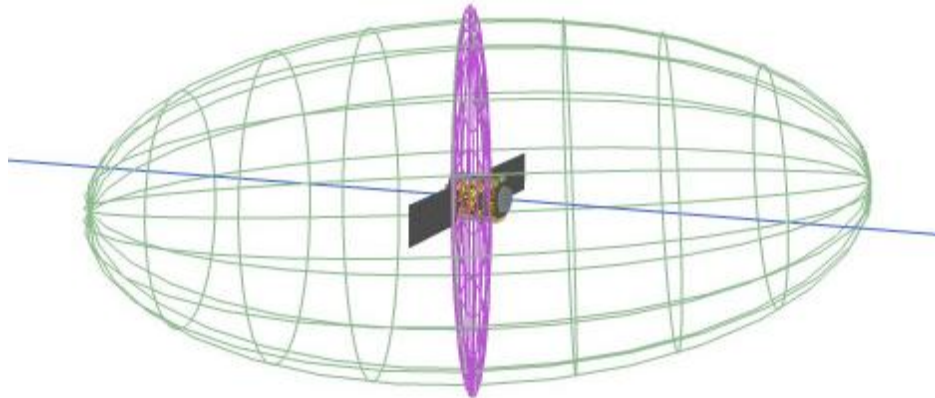


Figure 5. The relative position covariance ellipsoid, shown at a time just after a space based range measurement. The purple ellipsoid is computed with the cross correlation; the green one ignores the cross correlation.

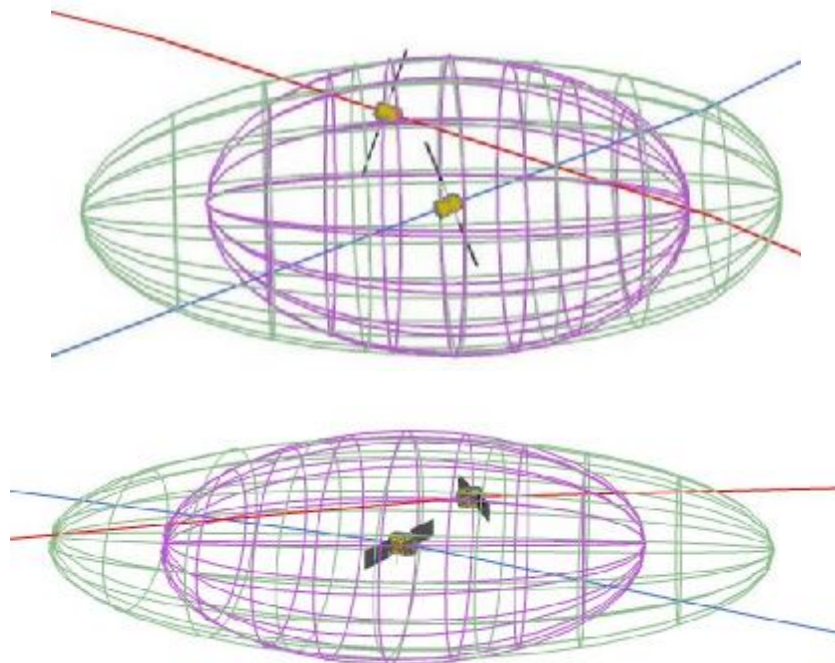


Figure 6. Two views of the same close approach event showing the relative position covariance ellipsoid. The purple ellipsoid is computed with the cross correlation; the green one ignores the cross correlation.